HIF1A contributes to the survival of aneuploid and mosaic pre-implantation embryos

Estefania Sanchez-Vasquez[1], Marianne E. Bronner[1] and Magdalena Zernicka-Goetz[1,2*]
[1]Division of Biology 139-74, California Institute of Technology, Pasadena, CA 91125, USA.
[2]Department of Physiology, Development and Neuroscience, University of Cambridge, Cambridge, UK.
*Lead and correspondence: magdaz@caltech.edu

Running title

HIF1A role in aneuploid and mosaic embryos

Key words

Embryogenesis/ Aneuploidy/ Mosaic embryos/ DNA repair/ Hypoxia

SUMMARY

Human embryos are often mosaics of diploid and aneuploid cells. We previously modeled elimination of aneuploid cells in pre-implantation mouse embryos using the Mps1 inhibitor reversine. Here, we develop an alternative model using AZ3146, a highly specific Mps1 inhibitor, to determine how aneuploid cells manage to survive within the mosaic embryos. We find that AZ3146 treated embryos overexpress Hypoxia-Inducible-Factor-1A (HIF1A), inhibition of which results in a decreased cell number of extra-embryonic trophectoderm but not embryonic epiblast cells. Hypoxia reduces the levels of DNA damage after either AZ3146 or reversine treatment, inferring a role of HIF1A in DNA repair. To analyze cell competition, we generated aggregation chimeras of DMSO-AZ3146-treated cells (low mosaics) and reversine-AZ3146-treated cells (medium mosaics). Both low and medium chimeras have similar number of cells at the blastocyst stage. However, diploid cells contribute preferentially to epiblast in low mosaics whereas AZ3146-treated cells outcompete reversine-treated cells in all the lineages of medium mosaics. Consistent with its proposed role in aneuploid survival, HIF1A downregulation in mosaic embryos reduces the number of aneuploid cells and favors development of diploid cells. Together these data indicate that diploid cells contribute preferentially to the epiblast and that the survival of aneuploid extra-embryonic cells is promoted by HIF1A.

INTRODUCTION

During fertilization, the sperm and egg combine to form a zygote, which subsequently undergoes a series of cleavage divisions as it travels through the fallopian tube to the uterus, where implantation occurs[1]. The zygote loses totipotency around the 2-4 cell stage, cells become polarized at the 8-cell stage and at the 8-32 cell stages, apolar cells are internalized to form the inner cell mass (ICM). The outer cells will differentiate into the trophectoderm (TE), which will give rise to the placenta, while the ICM will give rise to the primitive endoderm (PE) and epiblast (EPI) that sort into distinct layers in the blastocyst[1]. Intriguingly, the first zygotic

cleavage-stage divisions in human embryos are error prone, generally resulting in aneuploidy, in which cells gain or lose chromosomes[2-6].

Pre-implantation Genetic Testing for Aneuploidies (PGT-A) is a routine genetic screen of human embryos derived by *in vitro* fertilization to identify euploid embryos and select these for intrauterine transfer[7]. This procedure is important for detecting uniform aneuploidy (that can arise as a result of segregation errors in meiosis) and for detecting mosaic aneuploidy, common in cleavage-stage human embryos[8-10]. However, human mosaic embryos can develop to term[8-10]. Specifically, implantation of low-grade and medium-grade mosaic embryos (determined by biopsy of the TE) was as likely to result in the birth of healthy babies as implantation of fully euploid embryos[9].

Investigating chromosome mosaicism in human embryos faces ethical and technical barriers, but mouse models are amenable to such analyses. Recently, our group developed the first mouse model of chromosome mosaicism based on the generation of aneuploidies induced by a drug reversine[12,13], a pan-Aurora kinase inhibitor that also antagonizes the A3 adenosine receptor and inhibits mitotic kinase monopolar spindle 1 (MPS1)[14,15]. To generate a novel aneuploid model, here we use a more specific Mps1 inhibitor, AZ3146 that like reversine, interferes with the spindle assembly checkpoint[18] but binds to Mps1 in a different manner from reversine[20] and, as consequence, appears to generate a lower degree of aneuploidies[19,21]. AZ3146 is widely used for its effectiveness in generating specific trisomies in cancer lines to study metastasis[19,21]. Moreover, AZ3146 has been shown to double the occurrence of micronuclei (indicative of DNA damage and chromosome segregation defects) in mouse embryos but without negatively affecting cellular fitness[22]. In the present study, we use AZ3146 to generate a new model of aneuploid embryos and, combine this with our previous aneuploid reversine-based method, to help uncover the mechanisms underlying aneuploid cell elimination and survival.

RESULTS

AZ3146-treated embryos as a novel model of aneuploid embryo development

Depending on the degree of chromosome abnormalities, aneuploidies can cause a broad range of stress responses[23,24]. Because of reversine's affects on p53 and possible negative impact on cellular fitness[14,15], we sought to generate a complementary aneuploid model using a more specific Mps1 inhibitor AZ3146[18]. To this end, we treated mouse embryos at the 4-to-8 cell stage transition with either AZ3146 (20uM), reversine (0.5uM), or DMSO carrier as a control (Fig. 1A), and then cultured the treated embryos to the late blastocyst stage (E4.5) to assess lineage specification (Fig. 1B). Immunofluorescence analysis with antibodies against CDX2 (TE), NANOG (EPI) and SOX17 (PE) showed that all three lineages segregated normally, and that embryo morphology was not affected (Fig. 1B).

When we quantified the number of cells in the embryos, we found that both reversine- and AZ3146-treated embryos had significantly fewer cells than controls, with an average of 79 cells and 82 cells compared to 93, respectively (***P<0.0001, **P<0.01, *P<0.05, Mann–Whitney U-test, n=28 per treatment). We attribute this difference to a reduction in cell numbers in the ICM using both drug treatments: on average, the EPI in control embryos had 15 cells, whereas the EPI in reversine- and AZ3146-treated embryos had only 10 and 11 cells, respectively. Similarly, cell numbers in the PE were also reduced from an average of 11 cells in control embryos to 9 (reversine) and 6 (AZ3146). Cell numbers of the TE lineages in the blastocyst were also reduced in reversine-treated embryos (average of 60 TE cells). However, in AZ3146-treated embryos, this was not the case as we found that on average there were 67 TE cells compared to a normal average of 68 cells in controls (Fig. 1C).

Micronuclei, which reflect DNA encapsulated outside of the nucleus, are a useful marker of chromosome segregation errors and aneuploidy[25]. To examine the possible presence of micronuclei in our treated embryos, we performed *in situ* chromosome counting[6] and found that the presence of micronuclei increased in the reversine- and AZ3146-treated embryos by an average of 75% and 62.5%, respectively - compared with only 12.5% in DMSO-treated embryos (Fig. 1D,E). We also noted a marked increase of micronuclei without centromeres (9.7%) and non-dividing cells (19.4%) in reversine-treated embryos, both indicative of chromosome instability, a phenomenon associated with DNA damage and cancer[26].

We have previously shown that whole reversine-treated embryos are not able to develop to term[12]. To determine the developmental potential of AZ3146-treated embryos versus reversine-treated embryos, we transferred them into opposite uterine horns of the same mouse. As an indicator of successful implantation, we counted deciduas, and development to day E9.5. We found that a fraction (8%) of reversine-treated embryos was able to develop decidua, but none were able to give rise to viable E9.5 embryos (Fig. S1A). In contrast, 30% of AZ3146-treated blastocysts developed deciduas and 21% developed to E9.5 stage (Fig. S1B). These results suggest that AZ3146-treated embryos have higher developmental potential than reversine-treated embryos.

HIF1A promotes the survival of aneuploid trophectoderm cells

In somatic cells, p53 activation is a hallmark of high dosage aneuploidy[27,28]. Accordingly, Regin *et al*[17] confirmed by bulk RNA-seq of aneuploid human embryos that the p53 pathway is upregulated in high dosage aneuploidies, whereas in low dosage human aneuploid embryos, the hypoxic pathway is overexpressed. To investigate potential relationships between hypoxia and aneuploidy in our models, we focused on Hypoxia-inducible factor 1A (HIF1A), a transcription factor activated during hypoxia[29], as a marker for activation of the hypoxic pathway.

111 First, we performed qPCR against *p53* and *Hif1a* at the morula and blastocyst stages, normalizing against
112 *Ppia* (Peptidylprolyl Isomerase A) mRNA to control against changes in metabolism in aneuploid embryos[30].
113 In agreement with our previous results[13], we found that *p53* expression at the morula stage was significantly
114 increased (7-fold) in reversine-treated embryos and persisted until the blastocyst stage (1.3-fold increase).
115 In contrast, *p53* expression in AZ3146-treated embryos was not elevated at these two stages (Fig. 2A)
116 (**P<0.01, *P<0.05, Mann–Whitney U-test). Interestingly, we found that *Hif1a* was overexpressed (3-fold)
117 in AZ3146-treated morula. To validate these observations, we assessed HIF1A protein levels by
118 immunofluorescence (Fig. 2B). Our data confirmed that nuclear HIF1A expression was increased at the
119 morula stage, and there was an increase in both cytoplasmic and nuclear HIF1A at the blastocyst stage
120 (***P<0.0001, **P<0.01, *P<0.05, Mann–Whitney U-test).
121
122 HIF1A is activated in aneuploid cancer cells and is crucial for their survival[31]. In addition, aneuploidy survival
123 is hypothesized to be related to adaptation to hypoxia[31]. To examine these relationships in the mouse
124 embryos, we used a chemical approach to down-regulate HIF1A at different stages of aneuploid
125 development. To deplete maternal HIF1A, we used PX-478[32], an FDA-approved drug which functions as
126 a dominant-negative agent. We also down-regulated zygotic HIF1A indirectly using IDF-11774[33], which is
127 widely used to inhibit assembly of freshly translated HIF1A protein. Zygotes treated with PX-478 (2uM) and
128 IDF-11774 (20uM) were cultured to blastocyst stage and then stained with DAPI (DNA) to reveal total cell
129 number and CDX2 to indicate the number of trophectoderm cells (Fig. S2A). We found that PX-478 resulted
130 in a reduction in the overall cell number in the blastocyst (Fig. S2B), an average of 53 and 49 cells in
131 embryos treated with DMSO and IDF-11774, respectively, but an average of 13 cells in embryos treated
132 with PX-478 (***P<0.0001, **P<0.01, *P<0.05, Mann–Whitney U-test).
133
134 Given that IDF-11774 has less effect on pre-implantation development (Fig. S2), we selected this drug to
135 investigate the consequences of downregulating HIF1A during aneuploid development. Lineage
136 specification was assayed by immunofluorescence using antibodies against CDX2, NANOG and SOX17 to
137 mark the TE, EPI and PE, respectively (Fig. 2C). We found that IDF-1174 treatment affected development
138 of AZ3146-treated embryos: it led to a reduction in the TE cell number by approximately 50% and in the PE
139 cell number by approximately 80% in comparison to control embryos (Fig. 2D). In contrast, EPI cell number
140 was less affected by IDF-11774 treatment, whereas reversine-treated embryos maintained their regular
141 phenotype of an overall reduction in cell number (***P<0.0001, **P<0.01, *P<0.05, Mann–Whitney U-test).
142 Taken together, our data suggest that TE and PE cells depend on HIF1A to tolerate aneuploidy, whereas
143 EPI cells may be using other mechanisms to survive.
144
145 **Inhibition of PARP1 rescues AZ3146-treated embryos**
146 Survival of aneuploid cells is correlated with DNA repair[34]. Importantly, HIF1A binds directly to the main
147 activator of DNA repair mechanisms, Poly (ADP-ribose) polymerase 1 (PARP1)[35], a chromatin-associated

148 enzyme that senses DNA damage and promotes DNA repair mechanisms upon binding to both single and
149 double stranded DNA breaks[36] and that is maternally deposited in embryos[36-38]. However, the role of the
150 complex HIF1A/PARP1 in pre-implantation embryos is unknown. Using immunofluorescence, we found that
151 PARP1 protein was specifically enriched in the EPI lineage in comparison to the PE and TE (Fig. S3A). We
152 validated our observations of the *Parp1* mRNA enrichment in the EPI by re-analyzing published scRNA-
153 seq data of mouse blastocysts[39]. Next, we sought to investigate the effect of PARP1 on development of
154 aneuploid embryos.
155
156 Earlier studies demonstrated that pharmacological inhibition of the PARP1 pathway prior to the morula
157 stage is lethal for mouse [40,41] and porcine embryos[42]. To circumvent this issue and reveal lineage-specific
158 effects, we first treated embryos with both Mps1 inhibitors to generate aneuploidy and then, at the late
159 morula stage, with 10uM of the FDA approved PARP inhibitor, Olaparib[43,44] (Fig. S3C). Assessment of
160 lineage allocation was performed by immunofluorescence of CDX2 (TE), NANOG (EPI) and SOX17 (PE)
161 (Fig. S3B). Interestingly, we found that chemical downregulation of PARP1 appeared to rescue the
162 development of AZ3146-treated embryos, as reflected by close to normalized cell numbers relative to
163 control (Fig. S3D). In contrast, PARP1 inhibition only reduced survival of EPI and PE cells in reversine-
164 treated embryos (reduction to 0.63 and 0.68 compared to DMSO treatment, respectively) (*$P<0.05$, Mann–
165 Whitney U-test). These data suggest that PARP1 might have a dual function during embryo development -
166 it can promote survival or death, depending on the context and level of DNA damage. This dual function is
167 similar to its activity in cancer cells[36].
168
169 **Hypoxia reduces DNA damage and enhances DNA repair pathways in aneuploid embryos**
170 It is known that hypoxic conditions improve survival of bovine and human embryos, especially with respect
171 to the quality of the blastocyst[45,46]. It has been suggested that the capacity to repair DNA damage is
172 enhanced under hypoxic conditions[47,48]. Given that many human embryos have some level of aneuploidy
173 and most clinics culture human embryos under hypoxic conditions[49], we sought to assess relationships
174 between development of aneuploid mouse embryos, hypoxic conditions and DNA damage and repair
175 capacity. To this end, we performed treatment with the Mps1 inhibitors reversine and AZ3146 as described
176 (Fig. 1A) and cultured embryos under normoxic (air, 20% O_2/5% CO_2) and hypoxic (5% O_2/5% CO_2)
177 conditions. We then analyzed the levels of the DNA repair marker: PARP1 and the levels of the DNA
178 damage marker: the phosphorylated form of H2A.X (γH2A.X) by immunofluorescence (Fig. 3A-B) at the 8-
179 cell stage and in the morula in diploid (DMSO treated) and aneuploid embryos (reversine and AZ3146
180 treated embryos).
181
182 Under normoxic and hypoxic conditions, at the 8-cell stage, aneuploid-generating treatments resulted in an
183 increase in γH2A.X levels (Fig. 3C-D). In normoxic conditions, the increase in γH2A.X levels was
184 maintained at morula stages, but was reduced in AZ3146-treated blastocyst and increased in reversine-

185 treated blastocyst γH2A.X (Fig. S4A-B). Interestingly, γH2A.X levels were markedly reduced at the morula
186 stage under hypoxic conditions (***P<0.0001, **P<0.01, *P<0.05, t-test). These results suggest that
187 enhancement in repair mechanisms occurs between the 8-cell and morula stages, consistent with previous
188 hypotheses[50]. Importantly, we found that PARP1 levels were affected by reversine-treatment in normoxic
189 and hypoxic conditions at the 8-cell stage (Fig. 3C-D). Yet, PARP1 levels were rescued at the morula stage
190 under hypoxic conditions (Fig. 3D). Surprisingly, hypoxia appeared to promote the cytoplasmic localization
191 of PARP1 (Fig. S4C). Although cytoplasmic PARP1 has been reported upon viral infection[51], this has not
192 been previously observed during pre-implantation development. Overall, our results indicate that both
193 reversine and AZ3146 result in DNA damage and that hypoxia facilitates DNA damage repair.
194
195 To understand how early enhancement of DNA repair under hypoxic conditions influences lineage
196 specification, we quantified cell number in all three lineages at the blastocyst stage. We found that both
197 reversine- and AZ3146-treated embryos were similar to controls, with an average of 65 cells and 69 cells
198 compared to 70, respectively (***P<0.0001, **P<0.01, *P<0.05, Mann–Whitney U-test, n>26 per treatment).
199 Similarly, cell numbers in the TE and EPI were maintained: from an average of 53 cells in control embryos
200 to 49 (reversine) and 55 (AZ3146) in the TE, to an average of 12 cells in control embryos to 11 (reversine)
201 and 11 (AZ3146) in the EPI. Interestingly, cell numbers in the PE lineage were still reduced in aneuploid
202 embryos, to an average of 5 cells in control embryos to 4 (reversine) and 3 (AZ3146). These results are in
203 concordance with previous results on human embryos[17], in which the PE was found to be more sensitive
204 to aneuploid stress such that hypoxia may not rescue its development.
205
206 **Lineage allocation and cell competition in mosaic aneuploid embryos**
207 Low-to-medium mosaicism is characterized by the presence of aneuploidy in fewer that 50% of the cells in
208 TE biopsies[9,52]. Particularly, low mosaic embryos have aneuploid cells with a low degree of aneuploidy
209 (diploid-aneuploid mosaicism) whereas medium mosaic embryos have some cells with a high degree of
210 aneuploidy (ploidy mosaicism)[53]. To model low- and medium-grade mosaic embryos, we generated 8-cell
211 stage aggregation chimeras consisting of aneuploid cells (generated by AZ3146 or reversine treatments)
212 and euploid cells. Reversine-treated cells previously have been shown to be eliminated in the ICM via
213 apoptosis at the mature blastocyst stage[12,54]. Thus, we hypothesized that chimeras consisting of four
214 AZ3146-treated cells and four DMSO-treated cells (50% of total of cells) would mimic low mosaicism
215 (DMSO/AZ3146 chimeras), whereas chimeras consisting of four AZ3146-treated cells and four reversine-
216 treated cells (50% of total of cells) would mimic medium levels of mosaicism (Reversine/AZ3146 chimeras)
217 (Fig. 4A).
218
219 To follow the fate of individual blastomeres, we used transgenic mouse lines with membrane markers:
220 mTmG[55] and E-cadherin[56]. Based on lineage allocation and number of cells, we found that low and medium-
221 degree mosaicism did not affect embryo morphology or cavitation (Fig. 4B). In addition, low-and medium-

222 mosaic embryos have comparable total cell number (Fig. 4D). Intriguingly, medium-high mosaics grown
223 under normoxia present significantly more EPI lineage than low mosaic (Fig. 4D). Quantification of the
224 proportion of AZ3146 cells in the chimeras in each lineage showed that, in low mosaic chimeras, DMSO
225 and AZ3146-treated blastomeres contributed similarly to the TE; 46.75% originated from AZ3146-treated
226 blastomeres. Whereas diploid (DMSO-treated blastomeres) cells were preferentially allocated to the ICM
227 lineages, AZ3146-treated cell lineage contributed only 28.57% of total of PE cells and 42.86% of total of
228 EPI cells (Fig. 4F). In contrast, we observed in medium-high mosaic chimeras an enrichment of AZ3146-
229 treated cells in the TE (63.5%) and EPI (78.4%), although they accounted for a lower proportion of the PE
230 (40%) (Fig. 4F), as if AZ3146-treated blastomeres outcompeted reversine-treated blastomeres in their
231 contribution to TE an epiblast lineages under normoxia.
232
233 Since hypoxia has a clear effect on aneuploid survival, next we sought to understand how low levels of
234 oxygen affect the above cell competition in our chimeras. Importantly, culture of our chimeras in hypoxia
235 did not affect embryo morphology, cavitation (Fig. 4C), or cell number (Fig. 4E). In low mosaics, cell
236 contribution between DMSO and AZ3146-treated blastomeres was overall not affected by hypoxia (Fig.
237 4G). Although DMSO and AZ3146-treated blastomeres contributed similarly to the TE, we noticed that
238 diploid cells were preferentially allocated to the EPI. Specifically, AZ3146-treated blastomeres comprised
239 49.06% of the TE, 33.3% of the EPI and 50% of the PE. In contrast, in medium mosaic chimeras cultured
240 under hypoxia, the contribution of reversine-treated cells increased compared to medium chimeras cultured
241 under normoxia (Fig. 4G). Specifically, AZ3146-treated blastomeres contributed similarly to the TE
242 (55.94%), EPI (50%) and PE (46.43%). These results confirmed that hypoxia changes the contribution of
243 aneuploid cells in a lineage-specific manner. Hypoxia favors the survival of aneuploid PE in low mosaics
244 and favors the survival of reversine-treated cells in the medium-high mosaic embryos.
245
246 Next, we tested the correlation between the proportion of aneuploidy in the TE and the EPI in low and
247 medium-degree chimeras (Fig. S5A). We found an inverse correlation between the proportion of
248 aneuploidies cultured under normoxic conditions; DMSO/AZ have a coefficient of -0.39, and Rv/AZ have a
249 coefficient of -0.1366; these results were maintained in low mosaic embryos cultured in hypoxia (DMSO/AZ,
250 coefficient of -0.5955). These data are consistent with a preferential allocation of diploid cells to the EPI.
251 However, there is a direct correlation between aneuploid cells in medium mosaic embryos cultured in
252 hypoxia (Rv/AZ, coefficient of 1.2098). These data are consistent with an increased survival of reversine-
253 treated cells when medium mosaic chimeras are cultured under hypoxia.
254
255 Given that we did not observe preferential allocation of aneuploid cells to the TE when aneuploidy was
256 generated at the 4-to-8-cell stage, we next asked if lineage allocation was affected if aneuploidy was
257 generated earlier in development. Transcriptionally, lineage specification is initiated around the 2- to 4-cell
258 stage[57], such that generation of aneuploidy before lineage specification might influence lineage allocation.

259 To test this possibility, we assessed if treatment with reversine or AZ3146 during the first cell division
260 (zygote-2 cell) would affect lineage allocation (Fig. S6A). Although survival was reduced and blastocyst
261 development was impaired in reversine-treated embryos, neither survival nor lineage specification was
262 impacted by AZ3146 treatment (Fig. S6B) (n>27 per treatment, ***P<0.0001, **P<0.01, *P<0.05, Mann–
263 Whitney U-test).
264
265 Next, we generated aggregation chimeras at the 2-cell stage using transgenic lines with membrane
266 markers: mTmG and E-cadherin (Fig. S6C) and tested lineage allocation by immunofluorescence (Fig. S
267 6D). Considering that hypoxia influences the survival of aneuploid cells, we generated these chimeras
268 under normoxia. We found that 2-cell stage derived aggregation chimeras showed normal morphology and
269 cavitation (Fig. S7D). Interestingly, we observed an extrusion of the reversine-treated cells in the reversine-
270 DMSO chimeras (54% of the embryos) and reversine-AZ3146 (33% of the embryos), whereas no cell
271 extrusion was observed in the DMSO-AZ3146 chimeras. Quantification of the proportion of aneuploid cells
272 (AZ3146 or reversine) in 2-cell stage derived chimeras showed similar results as 8-cell stage derived
273 chimeras (Fig. S6E). In DMSO/AZ3146 chimeras, AZ3146-treated blastomeres were able to contribute
274 similarly to the TE, 49.28% but contributed only 33.33% of total of PE cells and 39% of total of EPI. In
275 contrast, reversine-treated blastomeres were again outcompeted by AZ3146 and DMSO-treated
276 blastomeres. In R/AZ3146 and DMSO/R chimeras, reversine-treated blastomeres contributed to the TE:
277 31.76%, 22.27%; to the PE: 33.33%, 26.98%; and to the EPI: 31.17%, 31.75%, respectively. These results
278 suggest that developmental timing does not affect allocation of aneuploid cells in the blastocysts
279
280 **Manipulating the development of mosaic aneuploid embryos**
281 Our data suggests that upregulation of HIF1A may confer tolerance to aneuploidy. To test this further, we
282 inhibited HIF1A in our AZ3146-DMSO (AZ-D) chimera and AZ3146-Reversine chimera (AZ-R) chimeras
283 with 20uM of IDF-11774 (Fig. 5A- S7A-B) and then assessed lineage allocation. In AZ-D chimeras,
284 treatment with IDF11774 impaired embryo cavitation (Fig. 5B,C). In AZ-R chimeras, not only cavitation but
285 overall embryo morphology was affected (Fig. 5E,F). In AZ-D chimeras, IDF-11774 caused a reduction of
286 the total number of cells (Fig. 5D), from 86 to 75 cells. This reduction arose from the reduction of the TE
287 from 65 to 55 cells on average. Importantly, IDF-11774 seemed to impair the contribution of AZ3146-treated
288 cells to all the lineages (Fig. S7 C). In the TE: 52.83% to 47.55%; in the PE: 44.12% to 32.3%; and in the
289 EPI: 41.6% to 33.25%. Intriguingly, in AZ-D chimeras, IDF-11774 treatments did not affect the number of
290 cells in the blastocysts (Fig. 5G). Yet, IDF-11774 increased the number of PE cells, from 6 to 8 on average.
291 Thus, IDF-11774 treatment appeared to affect the development of medium mosaic chimeras (Fig. S7B),
292 albeit the increase of the contribution of AZ3146-treated blastomeres was not statistically significant (Fig.
293 S7D, TE: from 56.08% to 59.69%; PE: from 57.2% to 59.25%; EPI: from 46.3% to 52.64%). Taken together,
294 our data support the possibility that down-regulation of HIF1A affects the survival of aneuploid cells in
295 chimeric embryos.

296

297 **DISCUSSION**

298 Aneuploidy is a common event during pre-implantation development due to a permissive SAC and
299 replication stress[2-4]. Here, we describe different strategies to study how the embryo responds to aneuploidy,
300 activates DNA repair mechanisms, tolerates chromosomal instability, and behaves in a mosaic context. Our
301 results indicate that: 1) the high specificity Mps1 inhibitor, AZ3146, can be used to generate aneuploid
302 embryos. 2) Lineage specific responses to aneuploidy are present during blastocyst development, as we
303 showed previously[12,13]. 3) HIF1A contributes to the survival of low degree aneuploid TE cells and PARP1
304 is responsible for survival of aneuploid EPI cells. 4) Hypoxia enhances DNA repair and favors the survival
305 of aneuploid cells in chimeric embryos. 5) Hypoxia affects aneuploid-diploid cell competition in mosaic
306 embryos, as results, cavitation is compromise.

307

308 Aneuploidy could arises during early cleavage stages [58] and has both immediate effects on cellular fitness
309 and long-term effects on subsequent cell cycles[23,24]. Once generated, and depending on the degree of
310 aneuploidy, an aneuploid blastomere is destined for either death, repair, or survival[59]. Reversine is known
311 to cause a high-dose of aneuploidy that activates apoptosis, which might not always represent what occurs
312 in the human embryos[17]. In mouse, reversine-treated embryos upregulate the senescent markers p53 and
313 p21[13] and thus fail to give rise to viable embryos[12]. Our results indicate that reversine also downregulates
314 PARP1, as previously observed in glioma[60]. Thus, the effect of reversine on embryo development can be
315 due to a combination of increase in DNA damage and downregulation of DNA repair. As an alternative
316 strategy to study aneuploidy, we introduced AZ3146-treatment[18] as a new model of aneuploidy in mouse
317 embryos. This has enabled us to discover that some aneuploid blastomeres overexpress HIF1A, have
318 increased survival of TE cells, and can survive to early post-implantation stages.

319

320 Considering that aneuploid human embryos upregulate hypoxic pathways[17], we sought to understand if
321 chemical inhibitors of HIF1A have an impact on aneuploid development. Our results demonstrate that down-
322 regulation of maternal HIF1A at the 8-cell stage is incompatible with blastocyst development. In contrast,
323 loss of zygotic HIF1A activity at the 8-cell stage interferes with TE survival in AZ3146-treated embryos. It is
324 known that p21/p53 pathways are incompatible with HIF1A by molecular competition for p300[61,62] and may
325 explain why reversine-treated embryos are not affected by downregulation of HIF1A. It is known that DNA
326 damage responses occur between the 8-cell and morula stages[38,59,63]. Accordingly, we find that PARP1
327 down-regulation at the 8-cell stage is incompatible with embryo survival[38,40]. However, chemical
328 downregulation of PARP1 during late morula stages affects the survival of EPI cells only when there is a
329 high dosage of aneuploidy. Due to an intrinsic role of maternally deposited HIF1A and PARP1, we are
330 unable to address the role of these proteins in aneuploid embryos at early stages. However, considering
331 the enrichment of PARP1 in the EPI, our results are consistent with previous reports suggesting that the
332 EPI lineage is more sensitive to aneuploidy and has a more regulated DNA damage response pathways

333 than the TE[17,52]. These findings further support the idea of lineage-specific responses to aneuploidy in the
334 blastocyst, as we previously discovered[12,13].
335
336 DNA repair pathways are enhanced under hypoxic environments in somatic cells[29,35,64]. Similarly, our data
337 show that aneuploid embryos cultured in hypoxia had lower levels of DNA damage at the morula stage, in
338 agreement with previous studies reporting that mouse blastocysts recovered from the uterus and
339 blastocysts cultured in hypoxia have lower levels of γH2A.X compared to cultures in normoxia[49,65]. Here,
340 we propose that hypoxia increases DNA repair mechanisms that will allow the aneuploid cells to survive
341 aneuploid stress. Interestingly, in cancer, recent studies suggest that hypoxia favors HIF1A's association
342 with PARP1[29,35,64] to increase DNA repair. We show that cytoplasmic PARP1 is present at morula stages
343 under hypoxia, a novel observation as the role of cytoplasmic PARP1 has only been described during DNA
344 damage caused by viral infections[51].
345
346 Confined placental mosaicism, commonly observed in human pregnancies, refers to instances where the
347 karyotype of the placenta is aneuploid and the karyotype of the fetus is euploid[53]. This phenomenon suggest
348 that unknown biological mechanisms preferentially allocate aneuploid cells to the placenta or aneuploid
349 cells can survive in the TE lineage contributing to the placenta. Our results show that highly aneuploid cells
350 upregulate p53[17,27] and, in mouse chimeric embryos, these cells are consequently eliminated from the
351 blastocyst stage onwards[12,13]. Unexpectedly, however, we found that in chimeras with a low degree of
352 aneuploidy, aneuploid cells are not only capable of surviving, but also make equal contributions towards
353 the TE lineage compared to control cells. In agreement with our previous work[12], none of our models
354 showed preferential allocation of aneuploid cells to the TE. Importantly, by generating aneuploidy with the
355 two different Mps1 inhibitors reversine and AZ3146, we modelled different degrees of mosaic aneuploidy
356 in embryos that represent low-to-medium- degrees of mosaicism. Overall, we modeled three populations
357 of blastomeres with different fitness: diploid blastomeres (DMSO-treated), blastomeres able to survive
358 (AZ3146-treated) and senescent blastomeres (reversine-treated). Placing these cells side-by-side in the
359 embryos allowed us to understand how hypoxia enhances the survival of aneuploid cells, likely due to an
360 enhancement of DNA repair. In our AZ3146-reversine chimeras, AZ3146-treated blastomeres can
361 outcompete reversine-treated blastomeres. These results agree with the well-known relationships between
362 different degrees of aneuploidy/chromosomal instability and cellular fitness[24].
363
364 Finally, our results confirm a lack of correlation between the proportion of aneuploid cells in the EPI
365 compared to the TE. We explain these results due to lineage specific response to aneuploid stress: survival
366 in the TE but elimination from the ICM. These results are not surprising considering that in human mosaic
367 aneuploid embryos, the aneuploidy concordance rates between TE and ICM is very low (30–40%)[72]. Since
368 mosaics with low-to-medium degrees of aneuploidy have similar survival potency as fully euploid
369 embryos[8,9], understanding the molecular pathways involved in their survival may have translational

370 implications. Given that the extent and proportion of aneuploid cells in mosaic embryos are the factors that
371 impact survival, we propose that a reduction in aneuploid cells in the blastocyst will favor a successful
372 pregnancy. Here, we downregulated HIF1A as a strategy for reducing aneuploid cells number and found
373 that treatment with IDF-11774 increases the proportion of diploid cells in chimeras having a low-degree of
374 aneuploid cells but impairs the development of chimeras with a medium degree of aneuploid. Discovering
375 the mechanisms that lead to these different responses could generate strategies to improve embryo
376 survival. In sum, our study contributes to understanding the survival mechanism of aneuploid cells within
377 mosaic embryos.
378
379 **MATERIALS AND METHODS**
380 **Pre-implantation embryo culture**
381 Mice were maintained according to national and international guidelines. Four- to six-week-old B6SJLF1/J
382 female mice were injected with 7.5IU PMSG followed by 7.5IU hCG 48h later, to induce superovulation.
383 The females were then mated with B6CBAF1/J males or were indicated, with E-cadherin GFP or mTmG
384 transgenic males. Pre-implantation mouse embryos were recovered 24h and 48h after the hCG injection to
385 obtain zygotes and 4-cell stage embryos, respectively in M2 medium (Sigma, M7167). When recovery
386 zygotes, cumulus cells were removed with 0.3% hyaluronidase (Sigma, H4272) in M2. Embryos then were
387 culture in regular KSOM (Sigma. MR-106) at 37°C under 5% CO_2/air (Normoxia) or 5% CO_2/ 5% O_2 balance
388 with nitrogen (Hypoxia). B6SJLF1/J females and B6CBAF1/J males were obtained from JAX laboratories.
389 Females were received at 3-4 weeks of age and were maintained in the CALTECH animal facility, where
390 they were housed with 5 same-sex littermates on a 12 h light/12 h dark cycle with food and water *ad libitum*.
391 The temperature in the facility was controlled and maintained at 21 °C. All experimental procedures
392 involving the use of live animals, or their tissues were performed in accordance with the NIH guidelines and
393 approved by the Institutional Animal Care and Use Committee (IACUC) and the Institutional Biosafety
394 Committee at the California Institute of Technology (CALTECH). Reversine (Sigma, R3904), AZ3146
395 (Sigma, SML1427), PX-478 (Selleckchem, S7612), IDF-11774 (Selleckchem, S8771) and olaparib
396 (Selleckchem, S1060) were dissolved in DMSO (Sigma, D2650) before use to specific concentration. They
397 were respectively used at following final concentrations: 0.5uM, 20uM, 2uM, 20uM and 10uM. Control
398 embryos were incubated in the equivalent DMSO concentration. Drugs were dissolved in regular KSOM to
399 the concentration of use. DMSO concentration in media should never pass 0.4%.
400
401 **Immunofluorescence**
402 Embryos were fixed in 4% PFA (Thermo Scientific, AA47340) for 20 min at room temperature (RT).
403 Following by three washes with 0.1% Tween-20 (Sigma, P1379) dissolved in PBS (PBST). The embryos
404 were then permeabilized with 0.3%, Triton X-100 (Sigma, X100) in PBS. Washes were then performed
405 three times in PBST before embryos were transferred to blocking solution (3% BSA in PBS) for at least 3h
406 at RT. Incubation with primary antibodies was performed in blocking solution overnight at 4°C. Next day,

407 washes were performed three times in PBST before incubation with Alexa Fluor secondary antibodies
408 (Thermo Fisher Scientific, 1:500) in blocking solution for 2h. Washes were performed three times before
409 incubation with DAPI (Thermo Fisher Scientific) for 5 min. Washes after DAPI were perform two times in
410 PBST before the final incubation in M2. Embryos were then mounted in M2 micro-drops on 35 mm glass
411 bottom dish (MATTEK, P35G-1.5-14-C). Confocal imaging was carried out using Leica SP8, 40x objective,
412 1um Z-step. Image files were viewed and analyzed using ImageJ and IMARIS 9.9 software.
413 Primary antibodies used: mouse anti-CDX2 (Biogenex, 1:500), rabbit anti-NANOG (1:500; Abcam), goat
414 anti-SOX17 (1:300; R&D Systems), rabbit anti-HIF1A (1:300, Novusbio), mouse anti-PARP1 (1:500,
415 Proteintech) and rabbit anti- Phospho- Histone H2AX (1:500, R&D Systems).
416
417 ***In situ* chromosome counting**
418 For determination of aneuploidy, treated 8-cell stage embryos were synchronized in metaphase by 10h
419 treatment with 0.03ug/mL colcemid (Cayman, 15364) diluted in KSOM. Following by 1h treatment with
420 10uM Mg132 (Selleckchem, S2619) in KSOM. Finally, 1h treatment with 5uM dimethylenastron
421 (MedChemExpress, HY-19944) and 10uM Mg132 in KSOM. Synchronized embryos were then fix in 2%
422 PFA for 20 min, permeabilized with PBST for 15 min and blocked 3h at RT before incubation with human
423 anti-centromere protein antibody (1:300, Antibodiesinc 15-234) overnight at 4°C. Next day, three washes
424 with PBST were performed before 2h incubation with goat anti-Human secondary antibody, Alexa Fluor
425 647 (1:400, Invitrogen A-21445) in blocking solution. Washes were performed three times before 20 min
426 incubation with DAPI (1:500) and Alexa Fluor 488 Phalloidin (1:300, Invitrogen A12379). Washes then were
427 performed three times before clearing overnight with AF1 plus (Citifluor, AF1/DAPI-15). Embryos were then
428 mounted in AF1 plus micro-drops on 35 mm glass bottom. Confocal imaging was carried out using Leica
429 SP8, 60x objective, 0.5um Z-step. Image files were viewed and analyzed using ImageJ and IMARIS 9.9
430 software.
431
432 **Embryo transfers and post implantation recovery and biopsy**
433 Embryo transfer were performed as described previously[73]. CD1 females and vasectomizes CD1 males
434 were obtained from Charles River. Reversine and AZ3146-treated blastocyst were transfer into 2.5-days
435 pseudopregnant CD1 females. Around 16 AZ3146-treated embryos were transfer in the right uterine horn,
436 whereas around 16 reversine-treated embryos were transfer in the left uterine horn of the same female as
437 control. To evaluate implantation and embryo survival potency, uterine horns were recovered 5 days after
438 surgery. Deciduas were dissected and post implantation embryos at stage E9.5 were recovered into PBST
439 on ice. Embryos were fixed in 4% PFA at RT for 1 h, followed by washes through PBST before imaging.
440 Images were taken using an Olympus LS stereo microscope with a 10x objective. Uterine transfers were
441 performed in accordance with the NIH guidelines and approved by the Institutional Animal Care and Use
442 Committee (IACUC) and the Institutional Biosafety Committee at the California Institute of Technology
443 (CALTECH).

444

445 **qRT-PCR**

446 Around 14 to 17 morulas and blastocysts were collected for quantitative reverse transcriptase polymerase
447 chain reaction (qRT-PCR). Total RNA from morulas was obtained using the NucleoSpin RNA Plus XS kit
448 (Takara, 740990.10). Whereas total RNA from blastocyst was extracted using the Arcturus PicoPure RNA
449 Isolation Kit (Thermo Fisher, KIT0204). qRT-PCR was performed using the *Power* SYBR Green RNA-to-
450 CT 1-Step Kit (Applied Biosystems, 4389986) in a StepOne Plus Real-time PCR machine (Applied
451 Biosystems). The following program was used: 30 min 48 °C (reverse-transcription) followed by 10 min 95
452 °C followed by 45 cycles of 15 s 95 °C (denaturing) and 1 min 60 °C (annealing and extension). The ddCT
453 method was used to determine relative levels of mRNA expression, with Ppia as an endogenous control[30].
454 Primers were obtained from IDT.

Name	Sequence
p53_Fw	GTCACAGCACATGACGGAGG
p53_Rv	TCTTCCAGATGCTCGGGATAC
Hif1a_Fw	CCTGCACTGAATCAAGAGGTTGC
Hif1a_Rv	CCATCAGAAGGACTTGCTGGCT
Ppia_Fw	GAGCTCTGAGCACTGGAGAGA
Ppia_Rv	CCACCCTGGCACATGAAT

455

456 **Generation of chimeric embryos**

457 Chimeric embryos were generated following a previous publish protocol[74]. Briefly, wild-type, E-cadherin
458 GFP or mTmG 8-cell stage embryos were transfer to micro-drops of M2 after aneuploid treatment. Zona
459 pellucida was removed by treatment with acidic Tyrode's solution (Sigma, T1788). The embryos were then
460 incubated in Ca2+/Mg2+-free M2 (made in house) for 5min and then disaggregated into individual
461 blastomeres by gentle mouth pipetting. Low mosaic chimeras were form by aggregation of four and four
462 (1:1) of DMSO/reversine-treated blastomeres with AZ3146-treated blastomeres, respectively in KSOM.
463 Medium mosaic chimeras were form by aggregation of three DMSO-treated blastomeres, three AZ3146-
464 treated blastomeres and two reversine-treaded blastomeres in KSOM. Culture of the chimeras were
465 performed under normoxic and hypoxia condition in KSOM for 48 to reach blastocyst stage.

466 **Statistical analysis**

467 The statistical tests used are indicated in the corresponding figure legends. Calculations were carried out
468 in Microsoft Excel and data analysis and visualization in Prism 9 software. All graphs show mean values,
469 error bars: s.e.m.

470

471 **AUTHOR CONTRIBUTIONS**

472 E.S.V designed and conducted the experiments; analyzed the data and wrote the manuscript. E.S.V and
473 M.Z.G conceived the project and interpreted the data. M.E.B and M.Z.G supervised the study.

ACKNOWLEDGEMENTS

This work was supported by M.Z.G' National Institutes of Health R01 (R01HD101489) grant. E.S.V. is supported by a Pew Latin America fellowship. We thank the Life Science Foundation, specially to C. Lilliehook for invaluable comments and suggestions on the manuscript and Ariane Helou for copy editing the manuscript. Data analysis was performed in the Biological Imaging Facility, with the support of the Caltech Beckman Institute and the Arnold and Mabel Beckman Foundation.

DECLARATION OF INTERESTS

The authors declare that they have no conflicts of interest.

REFERENCES

1. Zhu, M., and Zernicka-Goetz, M. (2020). Principles of Self-Organization of the Mammalian Embryo. Cell *183*, 1467-1478. 10.1016/j.cell.2020.11.003.
2. Allais, A., and FitzHarris, G. (2022). Absence of a robust mitotic timer mechanism in early preimplantation mouse embryos leads to chromosome instability. Development *149*. 10.1242/dev.200391.
3. Palmerola, K.L., Amrane, S., De Los Angeles, A., Xu, S., Wang, N., de Pinho, J., Zuccaro, M.V., Taglialatela, A., Massey, D.J., Turocy, J., et al. (2022). Replication stress impairs chromosome segregation and preimplantation development in human embryos. Cell *185*, 2988-3007 e2920. 10.1016/j.cell.2022.06.028.
4. Currie, C.E., Ford, E., Benham Whyte, L., Taylor, D.M., Mihalas, B.P., Erent, M., Marston, A.L., Hartshorne, G.M., and McAinsh, A.D. (2022). The first mitotic division of human embryos is highly error prone. Nat Commun *13*, 6755. 10.1038/s41467-022-34294-6.
5. Vanneste, E., Voet, T., Le Caignec, C., Ampe, M., Konings, P., Melotte, C., Debrock, S., Amyere, M., Vikkula, M., Schuit, F., et al. (2009). Chromosome instability is common in human cleavage-stage embryos. Nat Med *15*, 577-583. 10.1038/nm.1924.
6. Pauerova, T., Radonova, L., Kovacovicova, K., Novakova, L., Skultety, M., and Anger, M. (2020). Aneuploidy during the onset of mouse embryo development. Reproduction *160*, 773-782. 10.1530/REP-20-0086.
7. Garcia-Pascual, C.M., Navarro-Sanchez, L., Navarro, R., Martinez, L., Jimenez, J., Rodrigo, L., Simon, C., and Rubio, C. (2020). Optimized NGS Approach for Detection of Aneuploidies and Mosaicism in PGT-A and Imbalances in PGT-SR. Genes (Basel) *11*. 10.3390/genes11070724.
8. Greco, E., Minasi, M.G., and Fiorentino, F. (2015). Healthy Babies after Intrauterine Transfer of Mosaic Aneuploid Blastocysts. N Engl J Med *373*, 2089-2090. 10.1056/NEJMc1500421.
9. Capalbo, A., Poli, M., Rienzi, L., Girardi, L., Patassini, C., Fabiani, M., Cimadomo, D., Benini, F., Farcomeni, A., Cuzzi, J., et al. (2021). Mosaic human preimplantation embryos and their developmental potential in a prospective, non-selection clinical trial. Am J Hum Genet *108*, 2238-2247. 10.1016/j.ajhg.2021.11.002.
10. Starostik, M.R., Sosina, O.A., and McCoy, R.C. (2020). Single-cell analysis of human embryos reveals diverse patterns of aneuploidy and mosaicism. Genome Res *30*, 814-825. 10.1101/gr.262774.120.
11. Tosh, J., Tybulewicz, V., and Fisher, E.M.C. (2022). Mouse models of aneuploidy to understand chromosome disorders. Mamm Genome *33*, 157-168. 10.1007/s00335-021-09930-z.
12. Bolton, H., Graham, S.J.L., Van der Aa, N., Kumar, P., Theunis, K., Fernandez Gallardo, E., Voet, T., and Zernicka-Goetz, M. (2016). Mouse model of chromosome mosaicism reveals lineage-specific depletion of aneuploid cells and normal developmental potential. Nat Commun *7*, 11165. 10.1038/ncomms11165.

522 13. Singla, S., Iwamoto-Stohl, L.K., Zhu, M., and Zernicka-Goetz, M. (2020). Autophagy-mediated
523 apoptosis eliminates aneuploid cells in a mouse model of chromosome mosaicism. Nat Commun
524 *11*, 2958. 10.1038/s41467-020-16796-3.
525 14. Santaguida, S., Tighe, A., D'Alise, A.M., Taylor, S.S., and Musacchio, A. (2010). Dissecting the
526 role of MPS1 in chromosome biorientation and the spindle checkpoint through the small molecule
527 inhibitor reversine. J Cell Biol *190*, 73-87. 10.1083/jcb.201001036.
528 15. D'Alise, A.M., Amabile, G., Iovino, M., Di Giorgio, F.P., Bartiromo, M., Sessa, F., Villa, F.,
529 Musacchio, A., and Cortese, R. (2008). Reversine, a novel Aurora kinases inhibitor, inhibits
530 colony formation of human acute myeloid leukemia cells. Mol Cancer Ther *7*, 1140-1149.
531 10.1158/1535-7163.MCT-07-2051.
532 16. Rito, T., Naftaly, J., Gleicher, N., and Brivanlou, A.H. (2019). Self-correction of aneuploidy in
533 human blastocysts and self-organizing gastruloids. Fertility and Sterility *112*, e127.
534 10.1016/j.fertnstert.2019.07.452.
535 17. Marius Regin, Y.L., Edouard Couvreu De Deckersberg, Yves Guns, Pieter Verdyck, Greta
536 Verheyen, Hilde Van de Velde, Karen Sermon, Claudia Spits (2022). Aneuploidy triggers
537 autophagy and p53-mediated apoptosis and impairs second lineage segregation in human
538 preimplantation embryos. https://www.biorxiv.org/content/10.1101/2022.08.31.506009v1.
539 18. Hewitt, L., Tighe, A., Santaguida, S., White, A.M., Jones, C.D., Musacchio, A., Green, S., and
540 Taylor, S.S. (2010). Sustained Mps1 activity is required in mitosis to recruit O-Mad2 to the Mad1-
541 C-Mad2 core complex. J Cell Biol *190*, 25-34. 10.1083/jcb.201002133.
542 19. Vasudevan, A., Baruah, P.S., Smith, J.C., Wang, Z., Sayles, N.M., Andrews, P., Kendall, J., Leu,
543 J., Chunduri, N.K., Levy, D., et al. (2020). Single-Chromosomal Gains Can Function as
544 Metastasis Suppressors and Promoters in Colon Cancer. Dev Cell *52*, 413-428 e416.
545 10.1016/j.devcel.2020.01.034.
546 20. Lan, W., and Cleveland, D.W. (2010). A chemical tool box defines mitotic and interphase roles for
547 Mps1 kinase. The Journal of cell biology *190*, 21-24. 10.1083/jcb.201006080.
548 21. Sheltzer, J.M., Ko, J.H., Replogle, J.M., Habibe Burgos, N.C., Chung, E.S., Meehl, C.M., Sayles,
549 N.M., Passerini, V., Storchova, Z., and Amon, A. (2017). Single-chromosome Gains Commonly
550 Function as Tumor Suppressors. Cancer Cell *31*, 240-255. 10.1016/j.ccell.2016.12.004.
551 22. Vazquez-Diez, C., Paim, L.M.G., and FitzHarris, G. (2019). Cell-Size-Independent Spindle
552 Checkpoint Failure Underlies Chromosome Segregation Error in Mouse Embryos. Curr Biol *29*,
553 865-873 e863. 10.1016/j.cub.2018.12.042.
554 23. Giam, M., and Rancati, G. (2015). Aneuploidy and chromosomal instability in cancer: a jackpot to
555 chaos. Cell Div *10*, 3. 10.1186/s13008-015-0009-7.
556 24. Hintzen, D.C., Soto, M., Schubert, M., Bakker, B., Spierings, D.C.J., Szuhai, K., Lansdorp, P.M.,
557 Kluin, R.J.C., Foijer, F., Medema, R.H., and Raaijmakers, J.A. (2022). The impact of
558 monosomies, trisomies and segmental aneuploidies on chromosomal stability. PLoS One *17*,
559 e0268579. 10.1371/journal.pone.0268579.
560 25. Vazquez-Diez, C., Yamagata, K., Trivedi, S., Haverfield, J., and FitzHarris, G. (2016).
561 Micronucleus formation causes perpetual unilateral chromosome inheritance in mouse embryos.
562 Proc Natl Acad Sci U S A *113*, 626-631. 10.1073/pnas.1517628112.
563 26. Daughtry, B.L., and Chavez, S.L. (2016). Chromosomal instability in mammalian pre-implantation
564 embryos: potential causes, detection methods, and clinical consequences. Cell Tissue Res *363*,
565 201-225. 10.1007/s00441-015-2305-6.
566 27. Narkar, A., Johnson, B.A., Bharne, P., Zhu, J., Padmanaban, V., Biswas, D., Fraser, A., Iglesias,
567 P.A., Ewald, A.J., and Li, R. (2021). On the role of p53 in the cellular response to aneuploidy. Cell
568 Rep *34*, 108892. 10.1016/j.celrep.2021.108892.
569 28. Soto, M., Raaijmakers, J.A., Bakker, B., Spierings, D.C.J., Lansdorp, P.M., Foijer, F., and
570 Medema, R.H. (2017). p53 Prohibits Propagation of Chromosome Segregation Errors that
571 Produce Structural Aneuploidies. Cell Rep *19*, 2423-2431. 10.1016/j.celrep.2017.05.055.
572 29. Nakamura, H., Sekine, H., Kato, H., Masai, H., Gradin, K., and Poellinger, L. (2022). Hypoxia-
573 inducible factor-1alpha and poly [ADP ribose] polymerase 1 cooperatively regulate Notch3
574 expression under hypoxia via a noncanonical mechanism. J Biol Chem *298*, 102137.
575 10.1016/j.jbc.2022.102137.

30. Gu, Y., Shen, X., Zhou, D., Wang, Z., Zhang, N., Shan, Z., Jin, L., and Lei, L. (2014). Selection and expression profiles of reference genes in mouse preimplantation embryos of different ploidies at various developmental stages. PLoS One *9*, e98956. 10.1371/journal.pone.0098956.
31. Simoes-Sousa, S., Littler, S., Thompson, S.L., Minshall, P., Whalley, H., Bakker, B., Belkot, K., Moralli, D., Bronder, D., Tighe, A., et al. (2018). The p38alpha Stress Kinase Suppresses Aneuploidy Tolerance by Inhibiting Hif-1alpha. Cell Rep *25*, 749-760 e746. 10.1016/j.celrep.2018.09.060.
32. Zhao, T., Ren, H., Jia, L., Chen, J., Xin, W., Yan, F., Li, J., Wang, X., Gao, S., Qian, D., et al. (2015). Inhibition of HIF-1alpha by PX-478 enhances the anti-tumor effect of gemcitabine by inducing immunogenic cell death in pancreatic ductal adenocarcinoma. Oncotarget *6*, 2250-2262. 10.18632/oncotarget.2948.
33. Ban, H.S., Kim, B.K., Lee, H., Kim, H.M., Harmalkar, D., Nam, M., Park, S.K., Lee, K., Park, J.T., Kim, I., et al. (2017). The novel hypoxia-inducible factor-1alpha inhibitor IDF-11774 regulates cancer metabolism, thereby suppressing tumor growth. Cell Death Dis *8*, e2843. 10.1038/cddis.2017.235.
34. Weaver, B.A., and Cleveland, D.W. (2006). Does aneuploidy cause cancer? Curr Opin Cell Biol *18*, 658-667. 10.1016/j.ceb.2006.10.002.
35. Pietrzak, J., Spickett, C.M., Ploszaj, T., Virag, L., and Robaszkiewicz, A. (2018). PARP1 promoter links cell cycle progression with adaptation to oxidative environment. Redox Biol *18*, 1-5. 10.1016/j.redox.2018.05.017.
36. Huang, D., and Kraus, W.L. (2022). The expanding universe of PARP1-mediated molecular and therapeutic mechanisms. Mol Cell *82*, 2315-2334. 10.1016/j.molcel.2022.02.021.
37. de Murcia, J.M., Niedergang, C., Trucco, C., Ricoul, M., Dutrillaux, B., Mark, M., Oliver, F.J., Masson, M., Dierich, A., LeMeur, M., et al. (1997). Requirement of poly(ADP-ribose) polymerase in recovery from DNA damage in mice and in cells. Proc Natl Acad Sci U S A *94*, 7303-7307. 10.1073/pnas.94.14.7303.
38. Pacchierotti, F., Ranaldi, R., Derijck, A.A., van der Heijden, G.W., and de Boer, P. (2011). In vivo repair of DNA damage induced by X-rays in the early stages of mouse fertilization, and the influence of maternal PARP1 ablation. Mutat Res *714*, 44-52. 10.1016/j.mrfmmm.2011.06.010.
39. Deng, Q., Ramskold, D., Reinius, B., and Sandberg, R. (2014). Single-cell RNA-seq reveals dynamic, random monoallelic gene expression in mammalian cells. Science *343*, 193-196. 10.1126/science.1245316.
40. Imamura, T., Neildez, T.M., Thenevin, C., and Paldi, A. (2004). Essential role for poly (ADP-ribosyl)ation in mouse preimplantation development. BMC Mol Biol *5*, 4. 10.1186/1471-2199-5-4.
41. Osada, T., Ogino, H., Hino, T., Ichinose, S., Nakamura, K., Omori, A., Noce, T., and Masutani, M. (2010). PolyADP-ribosylation is required for pronuclear fusion during postfertilization in mice. PLoS One *5*. 10.1371/journal.pone.0012526.
42. Lee, H.R., Gupta, M.K., Kim, D.H., Hwang, J.H., Kwon, B., and Lee, H.T. (2016). Poly(ADP-ribosyl)ation is involved in pro-survival autophagy in porcine blastocysts. Mol Reprod Dev *83*, 37-49. 10.1002/mrd.22588.
43. Hou, X., Cai, C., He, Y., An, S., Zhao, S., Sun, H., and Yang, Y. (2022). Protective Effect of Minocycline Hydrochloride on the Mouse Embryonic Development Against Suboptimal Environment. Front Cell Dev Biol *10*, 799042. 10.3389/fcell.2022.799042.
44. Prasad, C.B., Prasad, S.B., Yadav, S.S., Pandey, L.K., Singh, S., Pradhan, S., and Narayan, G. (2017). Olaparib modulates DNA repair efficiency, sensitizes cervical cancer cells to cisplatin and exhibits anti-metastatic property. Sci Rep *7*, 12876. 10.1038/s41598-017-13232-3.
45. Nguyen, A.Q., Bardua, I., Greene, B., Wrenzycki, C., Wagner, U., and Ziller, V. (2020). Mouse embryos exposed to oxygen concentrations that mimic changes in the oviduct and uterus show improvement in blastocyst rate, blastocyst size, and accelerated cell division. Reprod Biol *20*, 147-153. 10.1016/j.repbio.2020.03.011.
46. Ciray, H.N., Aksoy, T., Yaramanci, K., Karayaka, I., and Bahceci, M. (2009). In vitro culture under physiologic oxygen concentration improves blastocyst yield and quality: a prospective randomized survey on sibling oocytes. Fertil Steril *91*, 1459-1461. 10.1016/j.fertnstert.2008.07.1707.

47. Calvo-Asensio, I., Dillon, E.T., Lowndes, N.F., and Ceredig, R. (2018). The Transcription Factor Hif-1 Enhances the Radio-Resistance of Mouse MSCs. Front Physiol *9*, 439. 10.3389/fphys.2018.00439.
48. Kaplan, A.R., and Glazer, P.M. (2020). Impact of hypoxia on DNA repair and genome integrity. Mutagenesis *35*, 61-68. 10.1093/mutage/gez019.
49. Houghton, F.D. (2021). HYPOXIA AND REPRODUCTIVE HEALTH: Hypoxic regulation of preimplantation embryos: lessons from human embryonic stem cells. Reproduction *161*, F41-F51. 10.1530/REP-20-0322.
50. Musson, R., Gasior, L., Bisogno, S., and Ptak, G.E. (2022). DNA damage in preimplantation embryos and gametes: specification, clinical relevance and repair strategies. Hum Reprod Update *28*, 376-399. 10.1093/humupd/dmab046.
51. Wang, F., Zhao, M., Chang, B., Zhou, Y., Wu, X., Ma, M., Liu, S., Cao, Y., Zheng, M., Dang, Y., et al. (2022). Cytoplasmic PARP1 links the genome instability to the inhibition of antiviral immunity through PARylating cGAS. Mol Cell *82*, 2032-2049 e2037. 10.1016/j.molcel.2022.03.034.
52. Regin, M., Spits, C., and Sermon, K. (2022). On the origins and fate of chromosomal abnormalities in human preimplantation embryos: an unsolved riddle. Mol Hum Reprod *28*. 10.1093/molehr/gaac011.
53. McCoy, R.C. (2017). Mosaicism in Preimplantation Human Embryos: When Chromosomal Abnormalities Are the Norm. Trends Genet *33*, 448-463. 10.1016/j.tig.2017.04.001.
54. Yang, M., Rito, T., Metzger, J., Naftaly, J., Soman, R., Hu, J., Albertini, D.F., Barad, D.H., Brivanlou, A.H., and Gleicher, N. (2021). Depletion of aneuploid cells in human embryos and gastruloids. Nat Cell Biol *23*, 314-321. 10.1038/s41556-021-00660-7.
55. Muzumdar, M.D., Tasic, B., Miyamichi, K., Li, L., and Luo, L. (2007). A global double-fluorescent Cre reporter mouse. Genesis *45*, 593-605. 10.1002/dvg.20335.
56. Christodoulou, N., Weberling, A., Strathdee, D., Anderson, K.I., Timpson, P., and Zernicka-Goetz, M. (2019). Morphogenesis of extra-embryonic tissues directs the remodelling of the mouse embryo at implantation. Nat Commun *10*, 3557. 10.1038/s41467-019-11482-5.
57. Goolam, M., Scialdone, A., Graham, S.J.L., Macaulay, I.C., Jedrusik, A., Hupalowska, A., Voet, T., Marioni, J.C., and Zernicka-Goetz, M. (2016). Heterogeneity in Oct4 and Sox2 Targets Biases Cell Fate in 4-Cell Mouse Embryos. Cell *165*, 61-74. 10.1016/j.cell.2016.01.047.
58. Lee, A., and Kiessling, A.A. (2017). Early human embryos are naturally aneuploid-can that be corrected? J Assist Reprod Genet *34*, 15-21. 10.1007/s10815-016-0845-7.
59. Khokhlova, E.V., Fesenko, Z.S., Sopova, J.V., and Leonova, E.I. (2020). Features of DNA Repair in the Early Stages of Mammalian Embryonic Development. Genes (Basel) *11*. 10.3390/genes11101138.
60. Hirakata, C., Lima, K., De Almeida, B.O., De Miranda, L.B.L., Florencio, K.G.D., Furtado, L.C., Costa-Lotufo, L.V., and Machado-Neto, J.A. (2021). Targeting glioma cells by antineoplastic activity of reversine. Oncol Lett *22*, 610. 10.3892/ol.2021.12871.
61. Kilic Eren, M., and Tabor, V. (2014). The role of hypoxia inducible factor-1 alpha in bypassing oncogene-induced senescence. PLoS One *9*, e101064. 10.1371/journal.pone.0101064.
62. Obacz, J., Pastorekova, S., Vojtesek, B., and Hrstka, R. (2013). Cross-talk between HIF and p53 as mediators of molecular responses to physiological and genotoxic stresses. Mol Cancer *12*, 93. 10.1186/1476-4598-12-93.
63. Newman, H., Catt, S., Vining, B., Vollenhoven, B., and Horta, F. (2022). DNA repair and response to sperm DNA damage in oocytes and embryos, and the potential consequences in ART: a systematic review. Mol Hum Reprod *28*. 10.1093/molehr/gaab071.
64. Marti, J.M., Garcia-Diaz, A., Delgado-Bellido, D., O'Valle, F., Gonzalez-Flores, A., Carlevaris, O., Rodriguez-Vargas, J.M., Ame, J.C., Dantzer, F., King, G.L., et al. (2021). Selective modulation by PARP-1 of HIF-1alpha-recruitment to chromatin during hypoxia is required for tumor adaptation to hypoxic conditions. Redox Biol *41*, 101885. 10.1016/j.redox.2021.101885.
65. Meuter, A., Rogmann, L.M., Winterhoff, B.J., Tchkonia, T., Kirkland, J.L., and Morbeck, D.E. (2014). Markers of cellular senescence are elevated in murine blastocysts cultured in vitro: molecular consequences of culture in atmospheric oxygen. J Assist Reprod Genet *31*, 1259-1267. 10.1007/s10815-014-0299-8.

685 66. Brosens, J.J., Bennett, P.R., Abrahams, V.M., Ramhorst, R., Coomarasamy, A., Quenby, S.,
686 Lucas, E.S., and McCoy, R.C. (2022). Maternal selection of human embryos in early gestation:
687 Insights from recurrent miscarriage. Semin Cell Dev Biol *131*, 14-24.
688 10.1016/j.semcdb.2022.01.007.
689 67. Barad, D.H., Albertini, D.F., Molinari, E., and Gleicher, N. (2022). IVF outcomes of embryos with
690 abnormal PGT-A biopsy previously refused transfer: a prospective cohort study. Hum Reprod *37*,
691 1194-1206. 10.1093/humrep/deac063.
692 68. Lin, P.Y., Lee, C.I., Cheng, E.H., Huang, C.C., Lee, T.H., Shih, H.H., Pai, Y.P., Chen, Y.C., and
693 Lee, M.S. (2020). Clinical Outcomes of Single Mosaic Embryo Transfer: High-Level or Low-Level
694 Mosaic Embryo, Does it Matter? J Clin Med *9*. 10.3390/jcm9061695.
695 69. Daughtry, B.L., Rosenkrantz, J.L., Lazar, N.H., Fei, S.S., Redmayne, N., Torkenczy, K.A., Adey,
696 A., Yan, M., Gao, L., Park, B., et al. (2019). Single-cell sequencing of primate preimplantation
697 embryos reveals chromosome elimination via cellular fragmentation and blastomere exclusion.
698 Genome Res *29*, 367-382. 10.1101/gr.239830.118.
699 70. Barbash-Hazan, S., Frumkin, T., Malcov, M., Yaron, Y., Cohen, T., Azem, F., Amit, A., and Ben-
700 Yosef, D. (2009). Preimplantation aneuploid embryos undergo self-correction in correlation with
701 their developmental potential. Fertil Steril *92*, 890-896. 10.1016/j.fertnstert.2008.07.1761.
702 71. Griffin, D.K., Brezina, P.R., Tobler, K., Zhao, Y., Silvestri, G., McCoy, R.C., Anchan, R., Benner,
703 A., Cutting, G.R., and Kearns, W.G. (2023). The human embryonic genome is karyotypically
704 complex, with chromosomally abnormal cells preferentially located away from the developing
705 fetus. Hum Reprod *38*, 180-188. 10.1093/humrep/deac238.
706 72. Dahdouh, E.M., and Garcia-Velasco, J.A. (2021). Embryos with mosaic results: busting the myth!
707 Reprod Biomed Online *43*, 1-2. 10.1016/j.rbmo.2021.04.015.
708 73. Bermejo-Alvarez, P., Park, K.E., and Telugu, B.P. (2014). Utero-tubal embryo transfer and
709 vasectomy in the mouse model. J Vis Exp, e51214. 10.3791/51214.
710 74. Eakin, G.S., and Hadjantonakis, A.K. (2006). Production of chimeras by aggregation of embryonic
711 stem cells with diploid or tetraploid mouse embryos. Nat Protoc *1*, 1145-1153.
712 10.1038/nprot.2006.173.
713

Figure 1| **Comparative analysis of lineage specification in aneuploid embryos generated by selective Mps1 inhibitors AZ3146 and reversine.** (A) Graphic representation of 4-cell embryos treated with DMSO (control) or Mps1 inhibitors reversine (0.5um) and AZ3146 (20um) to inactivate the spindle assembly checkpoint (SAC) and induce chromosome segregation errors. After washing, embryos were cultured to the mature blastocyst stage (E4.5) and analyzed for lineage specification. (B) Immunofluorescence imaging of well-known lineage markers CDX2 (TE), NANOG (EPI) and SOX17 (PE) reveals that overall embryonic morphology and cavitation is not affected by Mps1 inhibition. (C) Cell ratios for each lineage were normalized to DMSO treated control. Importantly, both reversine and AZ3146-treatments reduce the number of cells in the ICM, marked by NANOG and SOX17. Whereas the trophectoderm, marked by CDX2, is reduced only in the reversine-treated embryos. (n=28 per treatment) (***P<0.0001, **P<0.01, *P<0.05, Mann–Whitney U-test, error bars represent s.e.m). (D) *In situ* chromosome counting of 8 cell stage embryos after drug treatments. Representative images of individual embryos in the different treatments. DNA (white) is visualized by DAPI staining and kinetochores (red) by CREST antibody. PB (polar body), MN (micronuclei). Each chromosome presents 2 CREST dots. The large number is the cell ID and the smaller number indicates the number of chromosomes, “n”. Diploid blastomeres present 40 pairs of CREST dots. Phalloidin (cyan) was used for cell segmentation. (E) Quantification of the incidence of aneuploid events, designated as those with more than 2 chromosomes (MN>2chr), less than 2 chromosomes (MN<2chr), without kinetochores (MN-CREST) and non-dividing nucleus (ND cell). We observed an increase in MN following reversine and AZ3146 treatment. Importantly, reversine-treated cells have a higher number of ND cells and MN-CREST staining. (n=128 cell DMSO treatment, n=152 cells AZ3146 treatment, n=72 cells reversine treatment, ****P<0.00001, **P<0.01, *P<0.05, Mann–Whitney U-test, error bars represent s.e.m).

Figure 2 | **HIF1A inhibition affects the survival of trophectoderm cells in low-degree aneuploid embryos.** A) qPCR analysis of *p53* and *Hif1a* mRNA expression at morula and blastocyst stages reveals that *p53* is upregulated in Reversine-treated embryos and that *Hif1a* is upregulated in AZ3146-treated embryos at morula stages; 3 biological replicates and 2 technical replicates per experiment with each replicate having a minimum of 16 embryos (**P<0.01, *P<0.05, Welch’s t-test). B) Immunofluorescence against HIF1A (black) shows an increase in nuclear intensity in AZ3146-treated embryos at morula stages. At blastocyst stage, nuclear and cytoplasmic HIF1A are increased in AZ3146-treated embryos; normalization was based on DAPI staining (magenta). (C) Immunofluorescence analysis of lineage specification in blastocyst cultured with the HIF1A inhibitor IDF-11774 using antibodies against CDX2 (TE), NANOG (EPI) and SOX17 (PE). Importantly, IDF-11774 appears to affect cavitation of some AZ3146-treated embryos. (D) Lineage analysis at the blastocyst stage shows that TE and PE specification are affected by IDF-11774 treatment. Ratio of cells in each lineage in the blastocyst is normalized to DMSO treatment. (***P<0.0001, **P<0.01, *P<0.05, Mann–Whitney U-test, error bars represent s.e.m).

Figure 3 | **Hypoxia affects the levels of DNA damage during pre-implantation development.** Analysis of DNA damage and repair based on immunofluorescence against γH2A.X (phosphorylated form of H2A.X, white) and PARP1 (red), respectively. 8 cell stage (cultured 64 hours post hCG) and morula stage (cultured 74 hours post hCG) embryos under (A) normoxic or (B) hypoxic conditions after drug treatments. Intensity analysis shows that reversine and AZ3146 increase DNA damage at 8 cell stage through morula stage under (C) normoxic conditions. Importantly, reversine appears to downregulate PARP1 expression at 8 cell stage, which extends to morula stage embryos. Under (D) hypoxic conditions, DNA damage appears to be downregulated after the 8-cell stage. Interestingly, PARP1 expression is altered only at the 8-cell stage in reversine-treated embryos (***P<0.0001, **P<0.01, *P<0.05, t-test).

Figure 4 | **Modeling low- and medium-degree mosaicism during pre-implantation development.** (A) Eight-cell stage aggregation chimeras containing a 1:1 ratio of reversine/DMSO-treated and AZ314-treated blastomeres were created using transgenics lines with membrane markers: mTmG (green) and E-cadherin (white). We designate DMSO/AZ3146 chimeras as low-degree mosaicism, whereas Reversine/AZ3146 chimeras represent medium-degree mosaicism. Immunofluorescence for CDX2, NANOG, and SOX17 was performed to test lineage specification and allocation during (B) normoxia and (C) hypoxia. Lineage allocation quantification was based on the above markers. Importantly, D) in normoxia, low and medium chimeras have the same number of cells in all the lineages except the EPI. In addition, AZ3146-treated blastomeres outcompete reversine-treated blastomeres in medium mosaics in the TE and the EPI. E) Under hypoxia, both low and medium chimeras have similar number of cells in all the lineages. Yet, AZ3146-blastomeres do not outcompete reversine-treated blastomeres. Quantification of the contribution of AZ3146-treated blastomeres to the chimeras showed that, (F) under normoxia, low mosaic chimeras do not present preferential allocation of aneuploid cells in the TE. In contrast, AZ3146-treated blastomeres increased their contribution in medium chimeras, but only significantly on the EPI and the PE. (G) During hypoxia, low mosaic chimeras did not change their behavior. Confirming that, in low-degree mosaicism, there is a preferential allocation of diploid cells to the EPI. In medium mosaic chimeras, AZ3146-treated blastomeres contribute similarly to reversine-blastomeres to the TE and EPI but significantly increase contribution to the EPI. These results indicate that hypoxia favors the survival of high dosage aneuploid cells (Experiments were repeated in triplicate, ****P<0.00001, **P<0.01, *P<0.05, Mann–Whitney U-test, error bars represent s.e.m).

Figure 5 | **Manipulating cell competition in low- and medium-degree mosaic embryos.** (A) Since hypoxia improves the survival of aneuploid cells, we inhibited HIF1A by IDF-11774 in 8-cell stage aggregation chimeras. Immunofluorescence for CDX2, NANOG, and SOX17 was performed to test lineage specification and allocation. (B) HIF1A downregulation in low-degree mosaicism does not affect overall morphology but affects (C) cavitation. In contrast, (E) HIF1A downregulation in medium-degree mosaicism affects morphology, and (F) cavitation of the embryos. Lineage allocation quantification after IDF-1174 reveals a significant reduction of total cell number (D) in low-degree mosaicism as well as a reduction in cell number in the TE but not in the EPI and PE. In contrast, total cell number is not affected (G) in medium-degree mosaicism. However, IDF11-774 treatment appears to increase the cell number of the PE. These results show that HIF1A downregulation in hypoxic conditions differentially affects each type of mosaic embryos. Experiments were repeated in triplicate, **$P<0.005$, *$P<0.05$, Mann–Whitney U-test, error bars represent s.e.m.

Figure 1

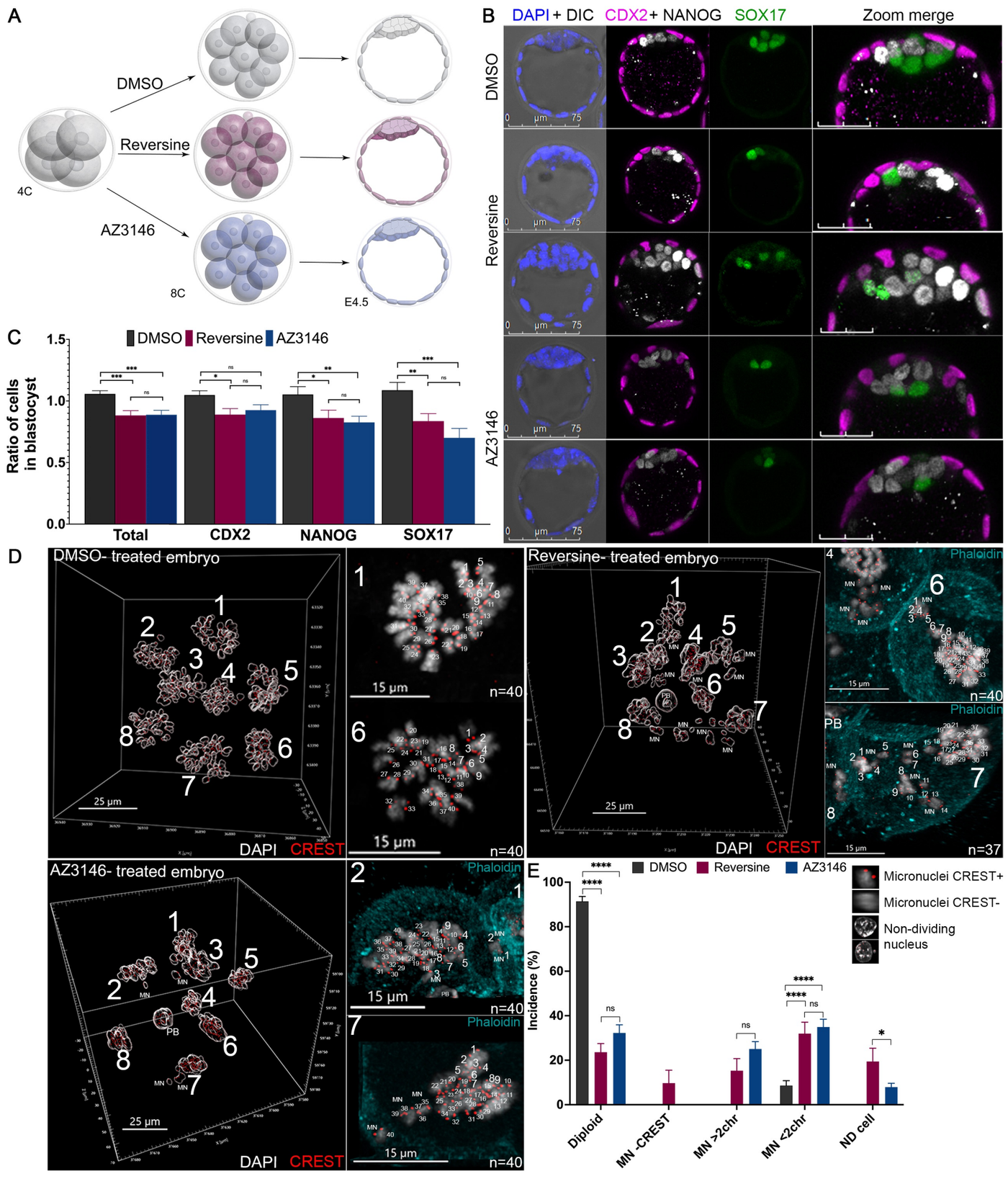
A
DMSO
Reversine
AZ3146
4C
8C
E4.5
B
DAPI + DIC
CDX2 + NANOG
SOX17
Zoom merge
DMSO
Reversine
AZ3146
C
DMSO
Reversine
AZ3146
Ratio of cells in blastocyst
Total
CDX2
NANOG
SOX17
D
DMSO- treated embryo
Reversine- treated embryo
AZ3146- treated embryo
25 µm
15 µm
n=40
n=37
DAPI
CREST
Phaloidin
PB
MN
E
DMSO
Reversine
AZ3146
Incidence (%)
Micronuclei CREST+
Micronuclei CREST-
Non-dividing nucleus
Diploid
MN -CREST
MN >2chr
MN <2chr
ND cell

Figure 2

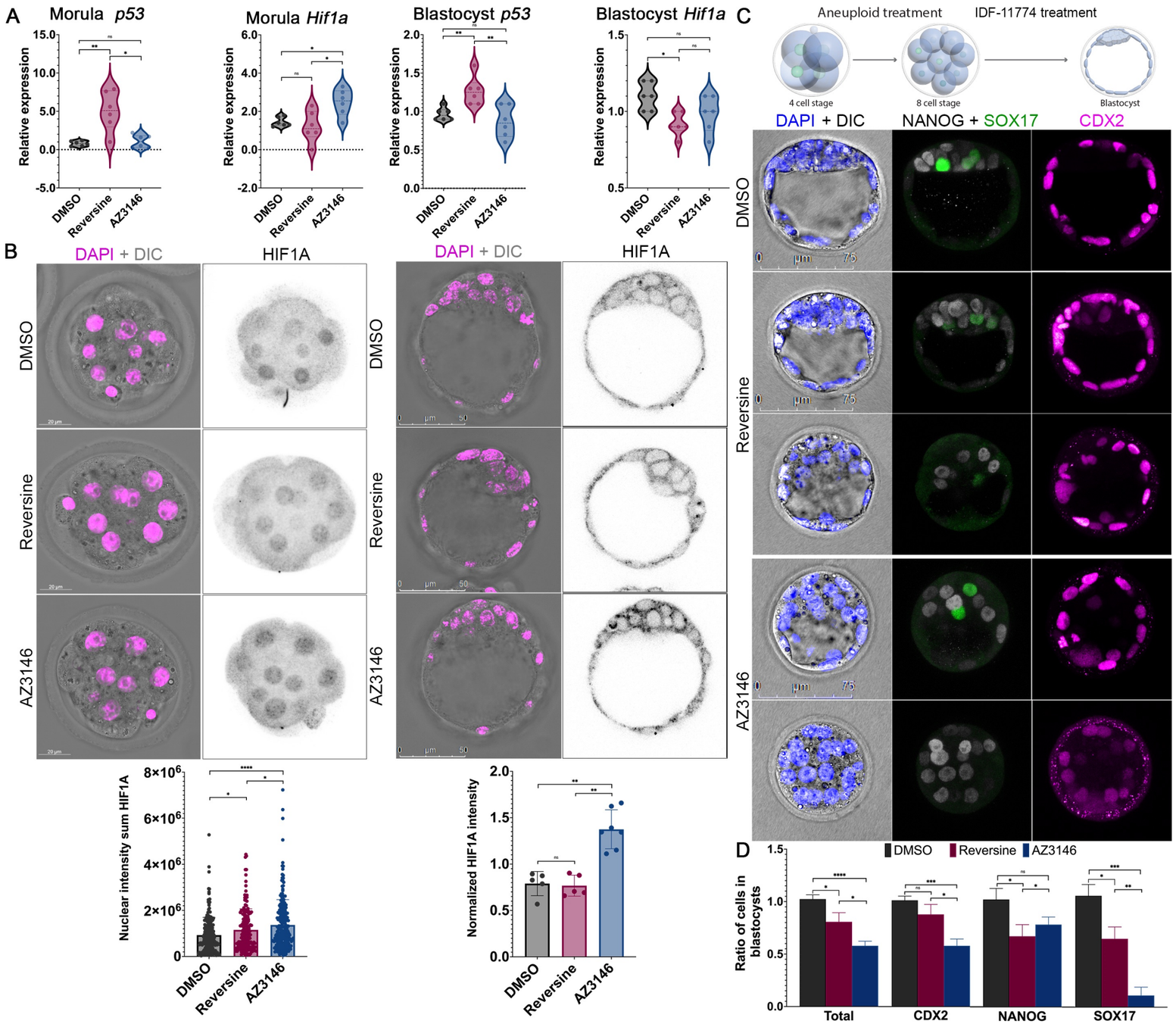
A
Morula p53
Morula Hif1a
Blastocyst p53
Blastocyst Hif1a
Relative expression
DMSO
Reversine
AZ3146
B
DAPI + DIC
HIF1A
DMSO
Reversine
AZ3146
Nuclear intensity sum HIF1A
Normalized HIF1A intensity
C
Aneuploid treatment
IDF-11774 treatment
4 cell stage
8 cell stage
Blastocyst
DAPI + DIC
NANOG + SOX17
CDX2
D
DMSO
Reversine
AZ3146
Ratio of cells in blastocysts
Total
CDX2
NANOG
SOX17

Figure 3

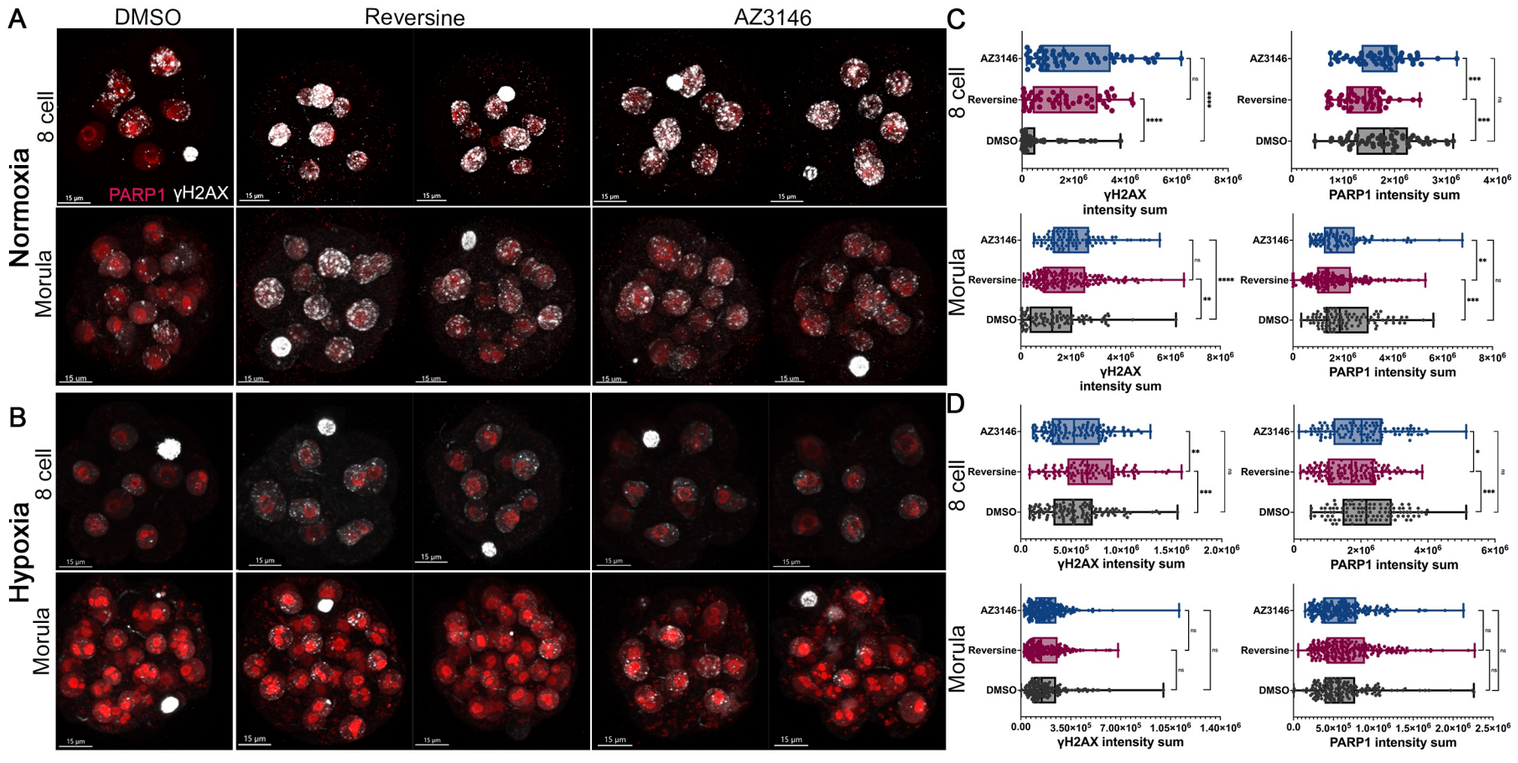
A
DMSO
Reversine
AZ3146
Normoxia
8 cell
Morula
PARP1 γH2AX
B
Hypoxia
C
D
AZ3146
Reversine
DMSO
γH2AX intensity sum
PARP1 intensity sum

Figure 4

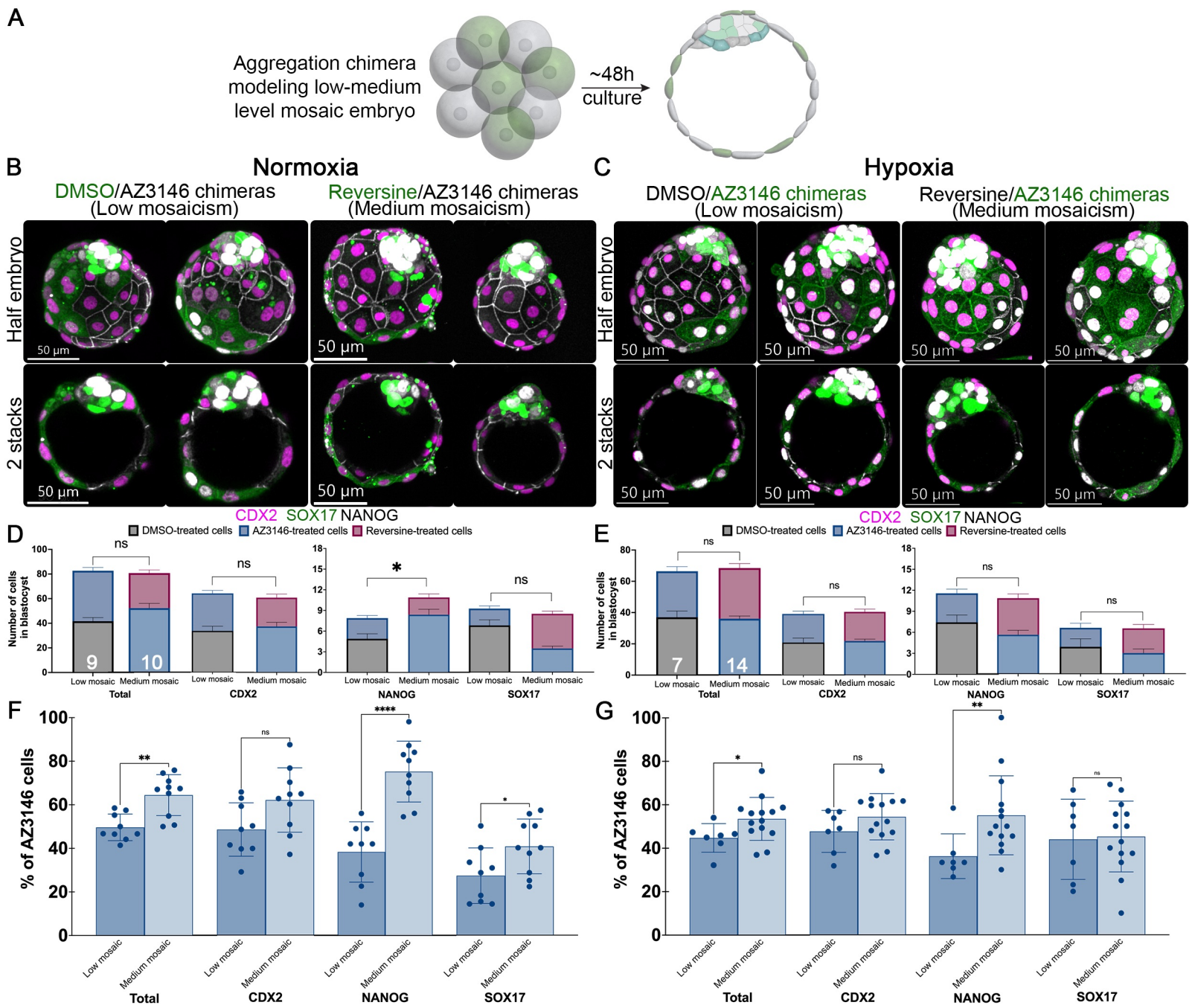
A
Aggregation chimera modeling low-medium level mosaic embryo
~48h culture
B
Normoxia
DMSO/AZ3146 chimeras (Low mosaicism)
Reversine/AZ3146 chimeras (Medium mosaicism)
Half embryo
2 stacks
50 µm
C
Hypoxia
DMSO/AZ3146 chimeras (Low mosaicism)
Reversine/AZ3146 chimeras (Medium mosaicism)
CDX2 SOX17 NANOG
D
E
DMSO-treated cells
AZ3146-treated cells
Reversine-treated cells
Number of cells in blastocyst
Low mosaic
Medium mosaic
Total
CDX2
NANOG
SOX17
F
G
% of AZ3146 cells

Figure 5

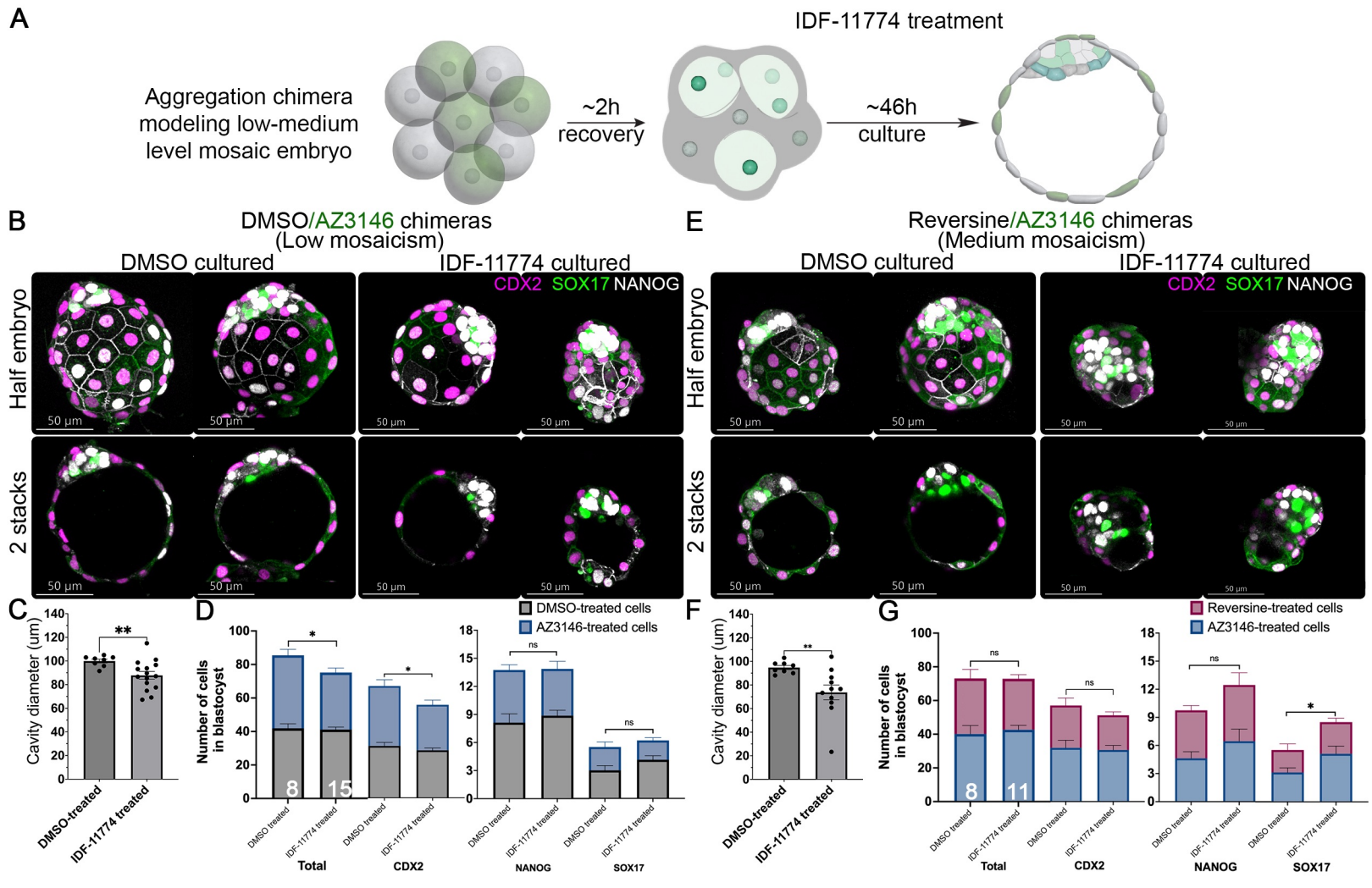
A
IDF-11774 treatment
Aggregation chimera modeling low-medium level mosaic embryo
~2h recovery
~46h culture
B
DMSO/AZ3146 chimeras (Low mosaicism)
DMSO cultured
IDF-11774 cultured
CDX2 SOX17 NANOG
Half embryo
2 stacks
50 µm
E
Reversine/AZ3146 chimeras (Medium mosaicism)
C
Cavity diameter (um)
DMSO-treated
IDF-11774 treated
D
DMSO-treated cells
AZ3146-treated cells
Number of cells in blastocyst
Total
CDX2
NANOG
SOX17
F
G
Reversine-treated cells
AZ3146-treated cells